Accuracy Comparison between Two Microcontroller-embedded R-wave Detection Methods for Heart-rate Variability Analysis

Toshitaka Yamakawa[1, 2, *], Ryunosuke Kinoshita[1], Koichi Fujiwara[3], Manabu Kano[3], Miho Miyajima[4], Tadashi Sakata[1], and Yuichi Ueda[1]
[1]Dept. of Computer Science and Electrical Eng., Graduate School of Science and Technology, Kumamoto University, Japan
[*]E-mail: yamakawa@cs.kumamoto-u.ac.jp, Tel: +81-96-342-3844
[2]Fuzzy Logic Systems Institute, Iizuka, Japan
[3]Dept. of Systems Science, Kyoto University, Kyoto 606-8501, Japan
[4]Tokyo Medical and Dental University, Tokyo, Japan

***Abstract*— Analysis of heart rate variability, which is calculated using the R–R intervals (RRI) of electrocardiogram (ECG), provides beneficial information for both clinical and healthcare diagnoses. To achieve the required accuracy for RRI measurement using the wearable telemetery system, two R-wave detection methods (one based on voltage threshold and another that adopts differential peak detection) were developed for implementation in a low-power microcontroller integrated into a wearable telemeter. Accuracy of these methods were compared using a clinical-grade ECG measurement system to evaluate the systematic errors of the proposed methods by correlation and Bland–Altman analyses.**

I. INTRODUCTION

Low cost methods of vital sign monitoring are in demand because of rapidly increasing healthcare costs. For early detection of diseases and acute symptoms, long-term monitoring of the electrocardiogram (ECG) delivers beneficial evidence for both clinical care and homecare. Analysis of heart rate variability (HRV), which is calculated using the R–R intervals (RRI), provides diagnostic evidences for arrhythmia [1], chronic obstructive pulmonary disease [2], and other diseases [3]. From the point of view of hardware implementation, RRI telemetry can be achieved by a lower power-consumption system compared with full-scale ECG telemetry.

Development of an HRV telemetry system described in this paper is ultimately for simple use, i.e., it offers high mobility and highly accurate detection of RRI. This telemeter is regarded as a consumer friendly device that can be commercially available at low cost and used by any subject without expert knowledge in ECG measurement. The telemetry system could be a supportive monitoring device because the collected data can be transferred as files of low size into the hospital's monitoring system for immediate diagnosis.

The accuracy of RRI measurement is crucial in obtaining reliable HRV indices. In this study, two R-wave detection methods were developed to be embedded in a low-power microcontroller. These developed programs were implemented in the telemeters comprising the same hardware structure, and their measurement accuracy was compared using a clinical-grade ECG measurement system to analyze the systematic errors.

II. SYSTEM DESCRIPTION

The developed RRI telemeter measures ECG, detects the R-waves from ECG, and transmits RRI data to a smartphone through Bluetooth wireless communication. The smartphone stores the received RRI data and calculates HRV indices. Details of the devices are explained in the following subsections.

Figures 1 (a) and (b) show the block diagram of the proposed RRI telemeter and the circuit diagram of the analog frontend, respectively. ECG measured using three electrodes (+, −, and GND) is amplified and conditioned in the analog frontend. To achieve a single power supply of 3.3 V DC, the common-mode feedback (CMFB) structure is adopted for the differential signal amplification as shown in the left dashed rectangle in Fig. 1 (b). The first-order variable-gain active low-pass filter (LPF) was designed to reduce high-frequency noise of >38 Hz. The output common-mode voltage of the analog frontend is set to V_{ref} because the positive nodes of OPAs are connected to V_{ref}. Here V_{ref} is given by a resistor chain to obtain the appropriate bias voltage of ECG baseline for the specific R-wave detection scheme as described in the following section. The current dissipation of the analog frontend was kept under approximately 80 μA by adopting the following low power ICs: INA122 for the instrumentation amplifier, MCP6042 for OPAs, and MCP4011 for the variable resistor. R_1 of 1 MΩ, R_2 of 1 MΩ, C_1 of 1μF, and C_2 of 4.7 nF were used in this prototype fabrication.

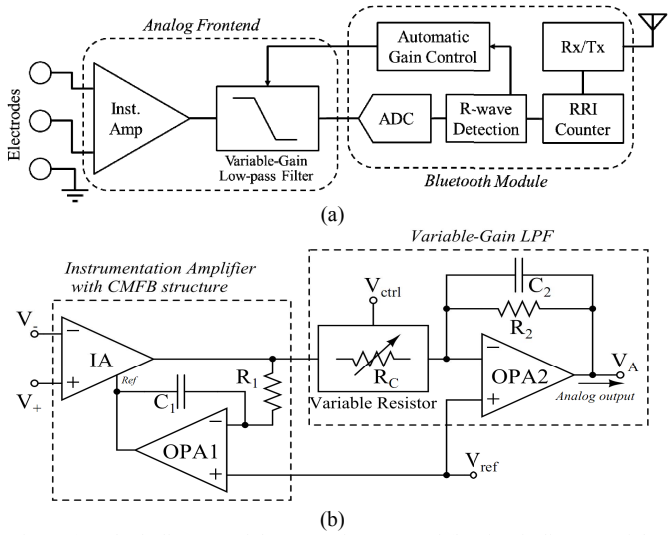

Fig. 1 (a) Block diagram of the RRI telemeter and (b) circuit diagram of the analog frontend.

The output of the analog frontend was connected to a Bluetooth-Smart Module (EYSFCNZXX, Taiyo Yuden), which is indicated as *Bluetooth Module* in Fig. 1 (a). The built-in microcontroller (Cortex M0, ARM) in the module observes ECG from the analog frontend, detects R-waves according to the methods described in the following section, and sends the derived R–R interval (RRI) data to a smartphone via the Bluetooth low energy wireless link using heart rate profile. The microcontroller also delivers the automatic gain control function [4], which can be operated by untrained subjects.

III. Embedded R-wave Detection Programs

The appropriately pre-processed ECG signal is fed to the input node of an analog-to-digital converter (ADC) built in the microcontroller, and is digitized to 10 bits of dynamic range with 1-kHz sampling frequency. The time of R-wave occurrence is extracted using one of the following two discrimination methods implemented in the microcontroller-embedded programs. As a preliminary trial, we developed two R-wave detection methods; simple voltage threshold discrimination and differential peak detection as described below.

A. Voltage Threshold

Simple threshold discrimination is a major candidate for R-wave detection because it can be implemented using minimal program memory. Furthermore, a voltage comparator circuit comprising an operational amplifier enables the omission of ADC. In this work, a voltage threshold discriminator with a quasi band-pass filter was developed for R-wave detection from ECG signal and was implemented in the microcontroller program.

Figure 2 (a) shows the basic principle of the proposed threshold-based discriminator. Here the ECG signal appears with an inverted waveform from the typical lead-II ECG because the variable-gain LPF has the negative feedback/input structure as shown in Fig. 1 (b).

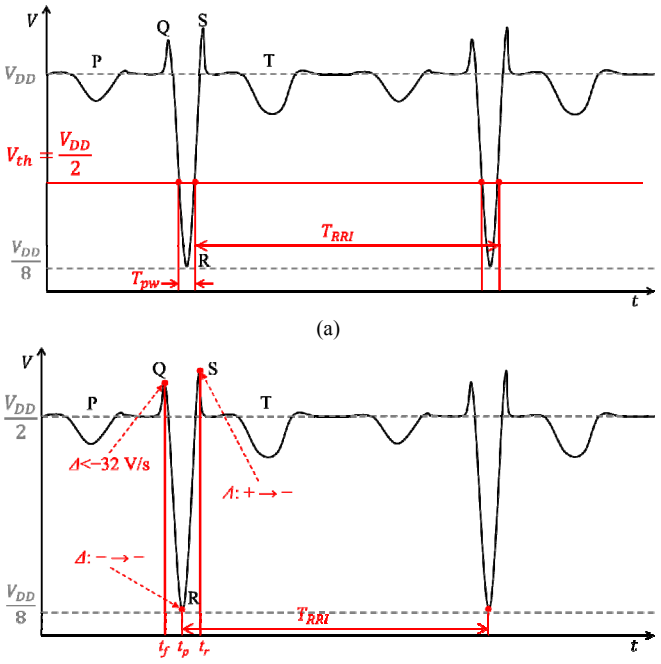

Fig. 2 Principle of R-wave detection using (a) voltage threshold and (b) differential peak detection. Capital Roman alphabets (P~T) indicate the naming of the waves in the ECG. The time points and durations are defined using small and capital italic letters, respectively.

The baseline and the negative peak voltages are set to be V_{DD} and $V_{DD}/8$, respectively, as shown by the gray lines in Fig. 2 (a) by the automatic gain control scheme performed at the beginning of the experiment. The built-in timer of the microcontroller counts the pulse width T_{pw} below the threshold voltage of $V_{DD}/2$. This pulse is estimated as an R wave when T_{pw} is in the range of 3–50 ms, which is determined using various human R-wave durations with a margin. Another built-in timer counts the pulse interval T_{RRI} at the rising edges of the R waves. When the derived T_{RRI} is between 200–1500 ms, it is determined to be an RRI and its value is transferred to the wireless transceiver block. Here the determination ranges of T_{pw} and T_{RRI} have been chosen by the study clinicians as part of a preliminary trial.

B. Differential Peak Detection

Peak detection using the first derivative of the ECG signal can be a solution for precise measurement of the peak point R waves. Figure 2 (b) shows the developed voltage differentiation method that can be performed by a Cortex M0 microcontroller. The baseline and the negative peak voltages are set to $V_{DD}/2$ and $V_{DD}/8$, respectively. The two adjacent values collected by the ADC ($v(t)$ and $v(t - T_S)$ where $v(t)$ is the voltage sampled at t and T_S is the sampling interval) are buffered in the memory, and their difference $\Delta = v(t) - v(t - T_S)$ is monitored. When the Δ is lower than −32 V/s, the point is defined as a falling edge t_f of an R-wave candidate. The sign of Δ is shifted from − to + after t_f is estimated as a peak point t_p of the R-wave candidate if the duration from t_f to t_p is in the range of 10–30 ms. After the detection of the peak point, a rising edge t_r is defined when the sign of Δ is shifted

from + to − where the duration from t_p to t_r is also in the range of 10–30 ms. If the falling edge, the peak point, and the rising edge are thoroughly elucidated using the above conditions, the R-wave candidate is determined as an R wave and the duration between the two adjacent t_p (indicated as T_{RRI} in Fig. 2 (b)) are transferd to the following RF block as an RRI.

IV. Experimental Results

The telemeter circuit was fabricated on a four-layer printed circuit board (PCB) of dimensions 45 × 29 mm, and was enclosed with a 110 mAh lithium-polymer rechargeable battery in a plastic case of 74 × 34 mm with a thickness of 12 mm. The two developed R-wave detection methods are separately implemented into two fabricated devices. The RRI data transmitted from the developed device was corrected by a dedicated Android application program installed in a Nexus 9 tablet. The reference ECG was acquired with a biomedical signal amplifier (AB-611J, Nihon Kohden) and a USB data acquisition system (Power Lab 16/35, AD Instruments), and was analyzed using the heart-rate variability toolbox of the data acquisition software (LabChart 8 Pro, AD Instruments).

The experiments were performed according to the protocols approved by the Research Ethics Committee of the Graduate School of Science and Technology, Kumamoto University and informed consent was collected from all participants.

For evaluating the measurement error of RRI, the fabricated devices and reference ECG were compared using simultaneous measurement of three healthy male subjects (21-22 years old) in a sitting position. Three disposable electrodes (Vitrode Bs-150, Nihon Kohden) were placed on the subject separately for each measurement device (i.e. 9 electrodes were used in total for a subject) in accordance with Lead II configuration to obtain the highest positive peak of R waves. The electrode locations were selected to avoid the large muscles such as pectoralis and abdominal oblique for minimizing the electromiyographic (EMG) contamination. The fabricated device with the thresholding detection, fabricated device with the peak detection, and reference ECG simultaneously collected RRIs of the resting subject in a sitting position for about 10 min as a measurement period. Three measurement periods were repeated on different days and the RRI data up to 3000 beats was collected and analyzed for each subject.

Figures 3 and 4 show the correlation plots with comparison of the fabricated devices and the reference for each subject. The dots and the red solid line show the data points and the regression line, respectively. The section filled in light red between the dashed red lines indicates the 95% Prediction Interval (PI) of the regression line. The outlier substantially deviating from the PI (such as the data points indicated with blue arrows in Figs. 3 and 4), which is presumably due to false detection of the R wave was excluded in the following analysis to evaluate the measurement difference separately from the false detection.

Although both fabricated devices had very good correlation with the reference equipment(0.9999, 0.9998, 0.9999 for Fig. 3 (a), (b), (c), and 0.9999, 0.9999, 0.9999 for Fig. 4 (a), (b),

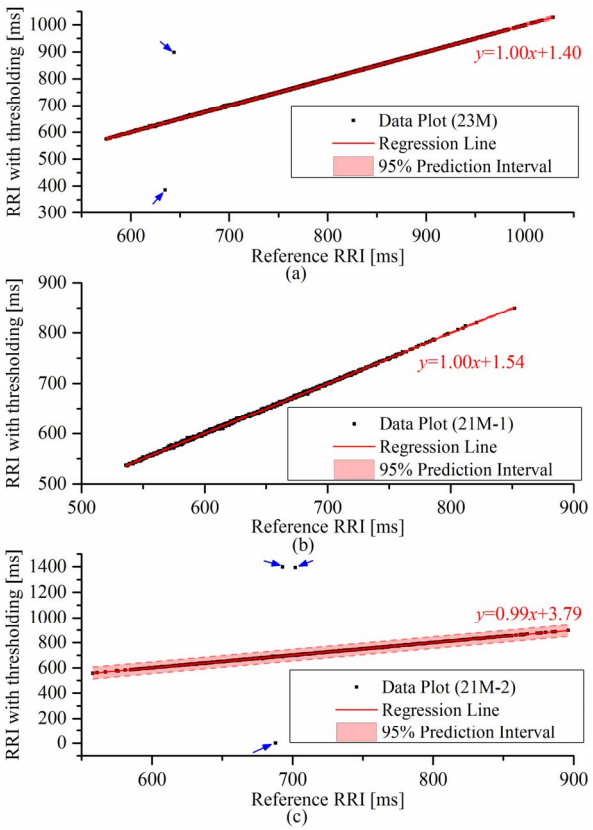

Fig. 3 Correlation plots between the fabricated device with the thresholding and the reference ECG for each subjects.

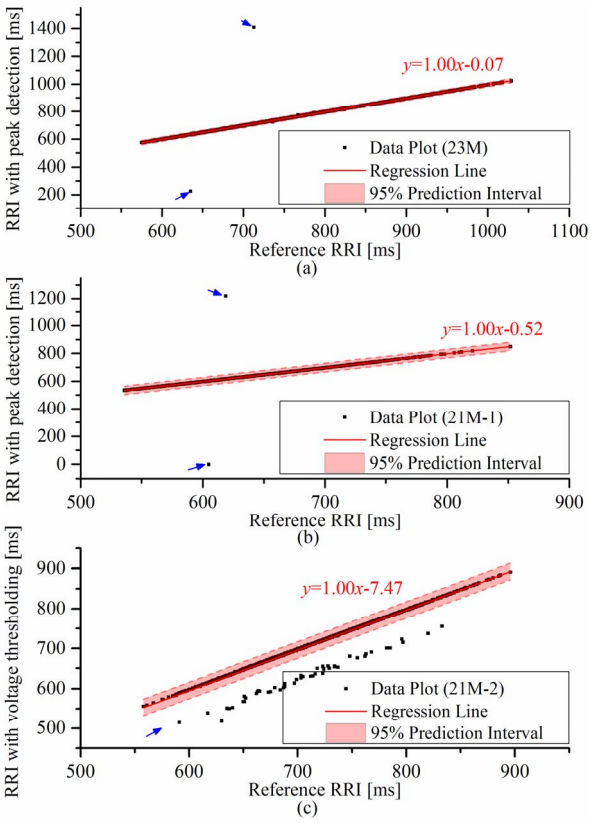

Fig. 4 Correlation plots between the fabricated device with the differential peak detection and the reference ECG for each subjects.

(c)), in the differential peak detection, an outlier group that constantly deviates to about 60 ms from the reference appeared in a subject as shown in Fig. 4 (c). The huge number of outliers were presumably caused by false detection of other ECG peaks such as P or T waves and certainly decreases the reliability of the calculated HRV indices. Therefore, the conditions of discrimination written in Sect. III-B should be tuned with a larger number of subjects when considering inter-subject ECG variance.

Bland–Altman plots [6] of the fabricated devices and the reference ECG are shown in Figs. 5 and 6. The horizontal and vertical axes are the mean and the difference (subtracting the device RRIs from the reference RRIs) of the compared systems. The blue dashed lines and the adjoining numbers indicate the mean of the difference. The blue solid lines are the intervals of the Limit Of Agreement (LOA, equals to 95% PI) of the measurement difference.

In the thresholding RRI measurement, the mean difference values indicated that the measurement bias of the device was sufficiently small, and the predictive measurement errors of about ±2 ms certainly satisfy the required accuracy for HRV analysis (better than ±4 ms) [3]. On the other hand, the measured RRIs with the peak detection method involved significant bias and considerable measurement errors. The fan-shaped plots shown in Fig. 5 also suggest that the method has a degree of proportional measurement error. Therefore, the systematic error cannot be denied in the proposed peak detection method.

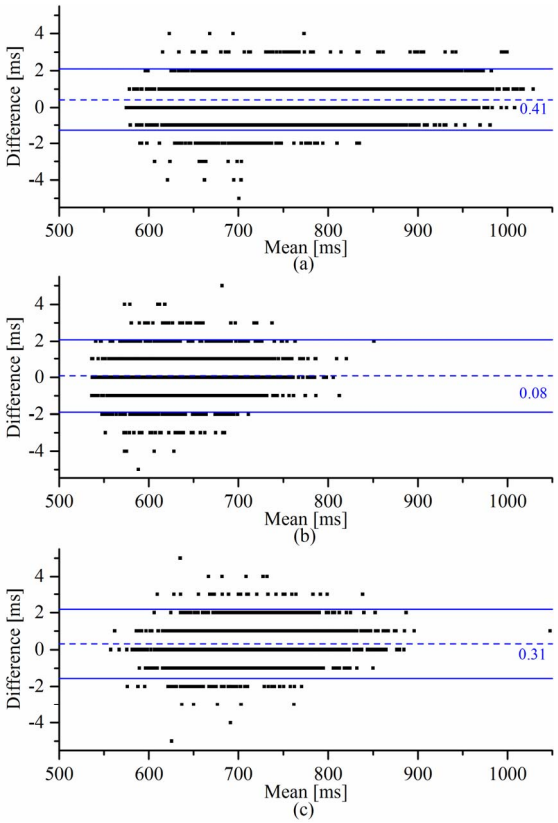

Fig. 5 Bland–Altman plots between the fabricated device with the thresholding and the reference ECG for each subject.

V. CONCLUSIONS

The two developed methods for R-wave detection from ECG implemented in the telemeter microcontroller programs have been evaluated for accuracy of RRI measurement. The RRI measured by the device with the threshold-based desclimination was consistent with the reference ECG sufficiently to the point that it could be used for HRV analysis. The results in the derivative-based peak detection method demonstrated that further tuning of the discrimination rules are necessary.

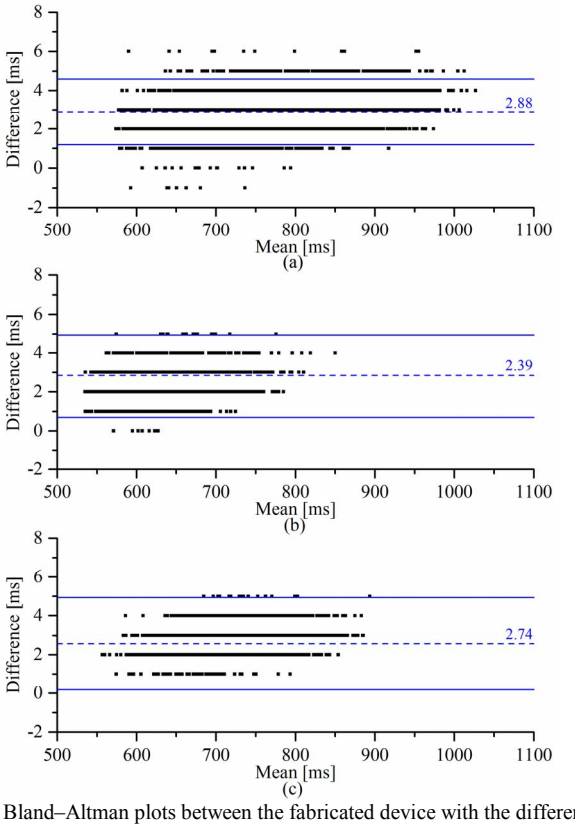

Fig. 6 Bland–Altman plots between the fabricated device with the differential peak detection and the reference ECG for each subject.

REFERENCES

[1] J. A. Taylor and D. L. Eckberg, "Fundamental Relations Between Short-term RR Interval and Arterial Pressure Oscillations in Humans," *Circulation*, vol. 93, no. 8, pp. 1527–1532, Apr. 1996.

[2] M. Pagani, D. Lucini, P. Pizzinelli, M. Sergi, E. Bosisio, G. S. Mela, and A. Malliani, "Effects of aging and of chronic obstructive pulmonary disease on RR interval variability," *Journal of the Autonomic Nervous System*, vol. 59, no. 3, pp. 125–132, Jul. 1996.

[3] Task Force of the European Society of Cardiology and the North American Society of Pacing and Electrophysiology, "Heart Rate Variability: Standards of Measurement, Physiological Interpretation, and Clinical Use," *Circulation*, vol. 93, no. 5, pp. 1043–1065, Mar. 1996.

[4] T. Yamakawa, G. Matsumoto, and T. Aoki, "A Low-Cost Long-Life R-R Interval Telemeter with Automatic Gain Control for Various ECG Amplitudes," *Journal of Advanced Research in Physics*, vol. 3, no. 1, 4 pages (available on-line), 2012.

[5] T. Yamakawa, K. Fujiwara, M. Miyajima, E. Abe, M. Kano, Y. Ueda, "Real-Time Heart Rate Variability Monitoring Employing a Wearable Telemeter and a Smartphone," *Proc. of APSIPA ASC 2014*, 2014.

[6] J. M. Bland, D. G. Altman, "Statistical Methods for Assessing Agreement Between Two Methods of Clinical Measurement," *The Lancet*, vol. 1, no. 8476, pp. 307–310, 1986.